Multi-Layer Feature Boosting Framework for Pipeline Inspection using an Intelligent Pig System

Hewu Xu[1], Yupei Yang[1], Bin Gao[1], Xiangyu Zhao, Wai Lok Woo[2]

[1]School of Automation Engineering, University of Electronic Science and Technology of China, China

[2]Department of Computer and Information Sciences, Northumbria University, England, UK.

Hewu Xu and Yupei Yang contribute equally. Corresponding author: bin_gao@uestc.edu.cn

Abstract— As pipelines take an increasingly important role in energy transportation, their health management is necessary. In-pipe inspection is a common pipeline life maintenance method. The signal obtained through internal inspection contains strong noise and interference where the internal environment of the pipeline is extremely complicated. Thus, it is challenging to accurately identify the defect signal. In this paper, a defect detection framework based on feature boosting is proposed by using the multi sensing pipeline pig as the detection signals. Through boosting construction of features and hierarchical classification, the framework can not only correctly classify various signals in the internal detection signals but also realize the accurate identification of defect signals. Concurrently, in order to demonstrate the high flexibility and robustness of the detection framework, experiments and verifications have been carried out on specimens in three different environments i.e., laboratory environment, simulated environment and actual environment. In the classification of actual environmental detection signals, quantitative evaluation with different algorithms have been undertaken using the F-score to demonstrate the effectiveness of the proposed framework.

***Index Terms*— In-pipe inspection, Feature Boosting, Time series anomaly detection, Multi-sensor fusion**.

I. Introduction

A time series is a collection of random variables indexed according to the order they are obtained in time [1]. It reflects the changing trend of one or more random variables over time, and describes the development of the phenomenon. Data mining is a significant meaningful method to obtain hidden information from time series for data analysis. Conventional data mining tasks can be divided into prediction, classification, clustering, correlation analysis, and anomaly detection.

Anomaly detection is an important part of data mining and it has diverse applications such as credit card fraud detection, network security intrusion detection, and industrial fault diagnosis. The aims are to find suspicious data caused by a different mechanism from majority of normal data. In the past few decades, many new models based on machine learning have been proposed for tackling the problem. Density-Based Spatial Clustering of Applications with Noise (DBSCAN) [2] is a density-based algorithm that can be used to identify anomalies. Local Outlier Factor (LOF) [3] proposes a local outlier factor to measure the degree of local isolation of data in anomaly detection. Anomalies are often quite different from normal data since there exists a natural way to distinguish anomalies by proximity, such as K-nearest neighbor (KNN) [4]. By using different hyperplanes to separate anomalies and normal values, One-Class support vector machine (OC-SVM) [5-7] has achieved good results in anomaly detection. Without relying on calculating distance or density, Isolation Forest (iForest) [8] can identify anomalies by measuring the concept of isolation, and the processing time is much shorter. Robust Random Cut Forest (RRCF) [9] improves iForest in which enabling real-time processing of data streams as well as anomaly detection. In addition, anomaly detection using deep networks has been well implementation. Both Long Short-Term Memory (LSTM) [10] and Autoencoder [11] learn the normal time series patterns and predict future values. By modeling the prediction error, an outlier score is given to identify anomalies. In high-dimensional data, a limited number of outliers may not provide sufficient information to help the classifier determine a boundary, so as to effectively separate the outliers from normal data. For this reason, Single-Objective Generative Adversarial Active Learning (SO-GAAL) and Multiple-Objective Generative Adversarial Active Learning (MO-GAAL) [11] can directly generate informative potential outliers based on the mini-max model between a generator and a discriminator. The existing time series anomaly detection methods are either applied to specific fields or require ideal conditions that are difficult to achieve in real application. To solve this problem, Mengran et al. [13] proposed a generic policy-based RL framework to address the time series anomaly detection problem. It gradually learns optimal policies from the interaction with time series data without above constraints. Anomaly detection on multivariate time-series still has serious limitations. When the relationship between different time series cannot be clearly obtained, this leads to erroneous interpretation and incorrect decision. To alleviate the situation, Zhao et al. [14] introduced graph attention layers to obtain the relationship of multivariate time series.

Non-destructive testing (NDT) belongs to a specific area of anomaly detection. It is a technique to evaluate the properties of a material, component or system without causing damage to the sample [15]. In-pipe inspection is an important field of NDT applications. Its purpose is to detect defects in the pipeline to avoid accidents such as pipeline leakage. In recent years, different NDT methods have been developed for in-line pipeline inspection. These are visual inspection[16], magnetic flux leakage (MFL) testing, ultrasonic testing (UT), electromagnetic acoustic technology (EMAT), eddy current testing (EC)[17]. Compared with other technologies, EC is sensitive to multiple parameters and can reflect defect characteristics[18]. At the same time, the size of the eddy current probe is small while it can be used to measure small diameter pipes[17]. Therefore, this paper chooses to use EC for in-pipe detection in the experiment.

Many methods have been proposed to detect anomalies in eddy current signals. Gupta et al. [19]fused the eddy current and the microwave signals while it used the Reed-Xiaoli (RX) algorithm and fuzzy logic-based algorithms to detect anomalies in the signal image. Sophian et al. [20] used Principal Component Analysis (PCA) to extract features of pulsed eddy current signals to detect abnormal signals. Ernest et al. [21] used the Gaussian sum method to generate Gaussian images and binarized them for anomaly detection where this proposed an automatic eddy current feature detection algorithm. D'Angelo et al. [22] used low definition Lissajous figures to extract features and performed automatic eddy current anomaly detection.

However, there are several shortcomings with the above methods. First of all, most of the above experiments only used one feature for anomaly detection and hence they did not fully exploit multiple features of the data. Secondly, the experimental settings are mostly carried out in a laboratory environment by using standard specimens where the obtained data is relatively ideal. Thus, the detection capability in the real environment becomes uncertain. Additionally, the model obtained by training is more complicated, and the training effect of the model depends on the settings of many hyperparameters, which leads to disadvantages of poor robustness and lower generalization of the model. Lastly, the process of the inner detector inside the pipeline is uncertain. This will generate interference signals such as jitter, stuck static, and lift-off that cover up the defect signal. Additionally, the internal environment of the pipeline is complex and subject to change such as variation due to high temperature and high pressure, and even the residues inside the pipeline are similarly affected. Substances can also have an effect on the internal detector signal, and interfering further the identification of defect signals. The pipeline contains various pipe-making mechanisms, such as welds, elbows, flanges, etc. The amplitude of the signal generated by these structures exceed the amplitude of the defect signal, and to worsen the situation, their waveforms are relatively similar to the defect signal. Since the interference signal of the pipe-making structure is not stripped, the cluttered signals containing multiple signals can lead to direct misclassification as defective signals as well as losing small defect information. Thus, this will cause significant false and missed detection of the defective signals. Fig. 1 illustrates the pig system conduction for the real running pipe.

Fig.1 (a)Complex pipeline scene. (b)Oil and residues. (c)Non-standard transceiver device. (d)Pigging valve

To ameliorate the above problems, this paper proposes the novel algorithm framework of features boosting structure, which adopts hierarchical feature engineering for gradually extracting the signal layer by layer. Each layer classifies the input complex signal through the extracted features, and divides it into the signal represented by the feature and the remaining signal. When the signal is input to the next layer from the previous layer, only the signal that has not been classified in the previous layer becomes the input. The complex signal is gradually decoupled in order to analyze the captured data in the real environment, and finally identify the target defect signal. This framework has the advantages of simplicity, efficiency, and extensible, which allows the system to achieve anomaly detection and classification through an end-to-end pipeline structure. Several experiments have been conducted and verified that the proposed framework has strong robustness and good generalization performance. In addition, for the challenge task for defective signal extraction, a new mathematical two-dimensional feature suitable for time series sequence is designed. It uses mathematical equations to map the time series to an image, whose two dimensions reflect the global and local characteristics of the sequence, respectively. Through a simple segmentation of this feature map, anomalous points in the time series can be easily found. In addition, it has a good representative effect for identifying most of the time series outliers. Three specimens in different environments were tested and trained. The results are compared with the current commonly used anomaly recognition algorithms.

In summary, the main contributions of this paper are as follows:

(i). A new framework for anomaly detection in time series is proposed. This framework has the advantages of simplicity, efficiency, and extensible, which allows users to achieve anomaly detection and classification through an end-to-end pipeline structure. Concurrently, a number of experiments have verified that the proposed framework has strong robustness and good generalization performance.

(ii). A new mathematical two-dimensional feature suitable for time series sequence is designed. It uses mathematical equations to map the time series to an image, whose two dimensions reflect the global and local characteristics of the sequence respectively. Through a simple segmentation of this feature map, anomalous points in the time series can be easily found. In addition, it has a good representative effect for identifying most of the time series outliers.

The rest of the paper is organized as follows: Section II describes the structure of the system as well as the collected information. Section III describes the proposed method with detailed interpretation. Experiments and result analysis are shown in Section IV. Finally, Section V summarizes the work and highlights future work.

II. RELATED WORK

In order to realize the detection of defects in pipeline, an in-pipe detector, known as the intelligent pig has been developed. Fig.2(a) shows the entire system which can be approximated as a cylinder. The circuit system is encapsulated in a cylindrical metal shell, which integrates Inertial Measurement Unit (IMU), data acquisition module, data processing module and communication module. A mileage wheel is installed behind the metal casing to record the distance for the system travels in the pipeline. A rubber sealed outer housing is installed on the outside of the shell, the diameter of which is equal to that of the pipe, so that the entire system can be placed close to the inner wall of the pipe. The eddy current sensor is encapsulated in an elastic material and combined to form a probe, and multiple probes adopt a petal structure to form a probe set. At the same time, the entire system uses two front and rear probe sets to achieve full coverage of the inner wall of the pipeline.

As shown in Fig. 2(b), when the intelligent pig is placed inside the pipeline, it will be pushed by the high-pressure gas from the rear to move inside the pipeline. With the movement of the intelligent pig, the petal-shaped probe will detect the pipe wall in real time. When a defect on the pipe wall is found, the signal received by the probe at the corresponding position will be significantly different from the background signal. This is characterized as the abnormal signal for detection. The petal-shaped probe can obtain both amplitude and phase signals. These are used for detecting defects through the changes of the collected signal. When the intelligent pig is running, the IMU integrated on the circuit board and the mileage wheel on the metal shell are also collecting data. Due to the residual magnetic field in the pipeline, the magnetometer cannot be used. However, this paper uses the MPU6050 six-axis sensor to calculate the attitude information of the intelligent pig. The distance obtained through mileage wheel can assist in the location of defects and verify the results. The signals obtained by the three sensors are depicted in Fig.2(c).

In terms of the different types of sensor signal interpretation, the inner detector consists of eddy current sensing probes with ten channels position at the front and another ten channels position at the back end, inertial measurement unit IMU and mileage encoder. Among them, the eddy current sensing probe is designed in the shape of a petal, and the probe is evenly distributed on the inner detector around the central axis. The inertial measurement unit IMU and the mileage encoder are integrated inside the inner detector. The eddy current probes proposed follow the principle of eddy current non-destructive testing to detect defects on the inner wall of the pipeline. Each probe will output the voltage amplitude and phase of the corresponding eddy current signal in real series, which contains information of defect, weld, pipe shape, and etc. The IMU is mainly used to measure the rotation angle of the inner detector system inside the pipeline, and the output signal is the nine-axis information output by the basic IMU. This is used for supporting clarification of weld, position and pipe elbow. The mileage encoder is used to measure the distance traveled by the inner detector in the pipeline, and the output signal is the number of pulses.

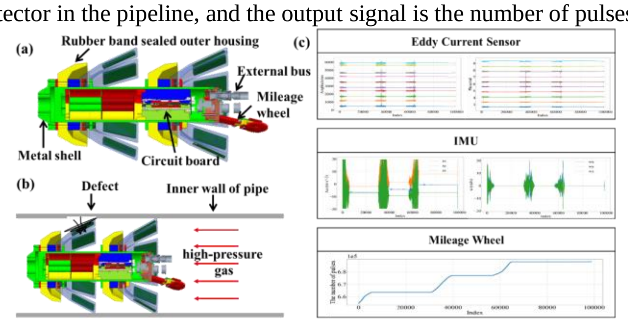

Fig. 2: Pipeline detection system. (a) Schematic diagram of an intelligent pig. (b) Schematic diagram of the work of the intelligent pig in the pipeline. (c) Signals collected by intelligent pig.

III. METHODOLOGY

In pipeline detection, the inner environment of the pipeline leads to complication of the received time series signal when it mixes with a variety of information. Taking eddy current sensing signal as example where it might consist of lift off impact from weld, dust interference, different kind of defects signals, to name a few. The question of how to gradually decouple this mixed signal and extract the target information is the purpose of the proposed layer feature boosting framework. The proposed framework draws on the idea of step boosting strategy. By selecting the appropriate features for boosting each step, the mixed time series can be decomposed into two parts at each step, the feature signal and the candidate residue. In the next round, new suitable features are selected to classify the previously unclassified candidate residue. After multiple rounds of feature iteration, a variety of information in the initial time series is extracted hierarchically.

This paper considers the real pipeline inspection as test platform. Through the time series signal collection, the layer feature boosting framework is used to extract pipeline defect information, pipeline status information (pipe bends, welds, ramps) and movement information (stationary and moving). Fig. 3 shows the overall structure of the proposed framework.

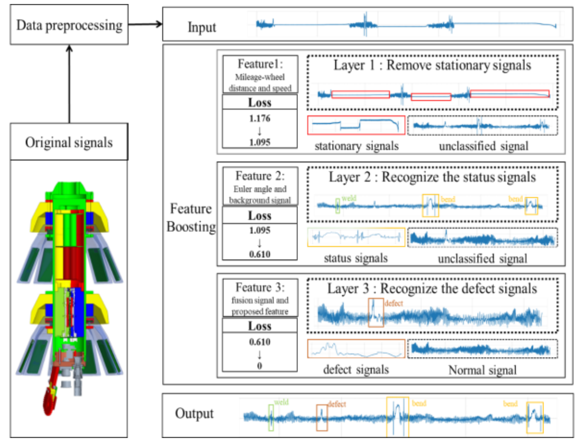

Fig.3 Proposed framework descriptions

A. Generative Model

As mentioned above, the signals collected in the real environment contain a variety of complex information. As such, this paper builds the following model to simulate the possible classification information detected in the pipeline:

$$
\begin{aligned}
\mathbf{w}_{MXN}(t) &= \mathbf{A}^{L}_{MxM}(t)\cdot\mathbf{S}_{MxN}(t)+R(L+1)\\
&=\begin{bmatrix} a^{j}_{11}(t) & a^{j}_{21}(t) & \cdots & a^{j}_{M1}(t)\\ a^{j}_{12}(t) & a^{j}_{22}(t) & \cdots & a^{j}_{M2}(t)\\ \vdots & \vdots & \ddots & \vdots\\ a^{j}_{1M}(t) & a^{j}_{2M}(t) & \cdots & a^{j}_{MM}(t)\end{bmatrix}\cdot\begin{bmatrix}\mathbf{S}(t) & \mathbf{S}(t) & \cdots & \mathbf{S}(t) & \mathbf{S}(t)\end{bmatrix}_{1xN}\\
&\quad +R(L+1)
\end{aligned}
\qquad (1)
$$

where $\mathbf{w}_{MXN}(t)$ represents the weight matrix calculated by the model at time t, M represents the number of signal categories that need to be classified, and N represents the number of sensor channels. $\mathbf{A}^{L}_{MxM}(t)$ represents the hierarchical matrix of the design at time t, and L represents the L-*th* layer in the frame. $\mathbf{S}_{MxN}(t)$ represents the typical signal matrix obtained after a large number of statistics, and $\mathbf{S}(t)$ in $\mathbf{S}_{MxN}(t)$ is a block matrix $\mathbf{S}(t)=[s_1 \quad s_2 \quad \cdots \quad s_{M-1} \quad s_M]^T$, in which s represents a typical signal. $R(L+1)$ represents the residual signal after the L-*th* layer classification, in other words, the $(L+1)$-*th* layer of the signal to be classified. When it comes to the final classification layer, $R(L+1)$ will usually be white noise.

B. Layer design

The key idea of layer feature boosting is to use different features to classify complex signals hierarchically. Therefore, when designing each layer structure, how to make the layer pay attention to the target signal of this layer is the focus of the design. With the help of the model in (1), we assume that the signal to be classified in the j-*th* layer is s_i. We can design the matrix $\mathbf{A}^{L}_{MxM}(t)$ of the j-*th* layer as:

$$\mathbf{A}_{M\times M}^{j}=\begin{bmatrix}0 & & & & \\ & \ddots & & & \\ & & a_{ii}^{j} & & \\ & & & \ddots & \\ & & & & 0\end{bmatrix}_{\mathrm{MxM}} \tag{2}$$

Combining (1) and (2), we can obtain the weight matrix $\mathbf{w}_{M\mathrm{xN}}^{t}$ of the j-th layer at time t as:

$$\begin{aligned}\mathbf{w}_{M\mathrm{xN}}^{t} &= \begin{bmatrix}0 & 0 & \cdots & \cdots & 0 & 0\\ 0 & 0 & \cdots & \cdots & 0 & 0\\ \vdots & \vdots & \vdots & \vdots & \vdots & \vdots\\ a_{ii}^{j}s_i & a_{ii}^{j}s_i & \cdots & a_{ii}^{j}s_i & a_{ii}^{j}s_i & a_{ii}^{j}s_i\\ \vdots & \vdots & \vdots & \vdots & \vdots & \vdots\\ 0 & 0 & \cdots & \cdots & 0 & 0\end{bmatrix}_{\mathrm{MxN}}\\ &= a_{ii}^{j}\begin{bmatrix}0 & 0 & \cdots & \cdots & 0 & 0\\ 0 & 0 & \cdots & \cdots & 0 & 0\\ \vdots & \vdots & \vdots & \vdots & \vdots & \vdots\\ s_i & s_i & \cdots & s_i & s_i & s_i\\ \vdots & \vdots & \vdots & \vdots & \vdots & \vdots\\ 0 & 0 & \cdots & \cdots & 0 & 0\end{bmatrix}_{\mathrm{MxN}}\end{aligned} \tag{3}$$

From (3), it can be seen that the focus of the model is on the target signal s_i at time t. For the entire time series ($t=1,2,\ldots,T$), there is an attention vector $\mathbf{W}_j$ for the attention signal s_i of the j-th layer. This extracts the effective data in the attention matrix $\mathbf{W}_j$ by using a classifier to determine whether it belongs to the attention signal s_i, and obtain the classification result vector $\mathbf{C}_{TxN}^{j}$. $\mathbf{C}_{TxN}^{j}$ is an index whether the time series in the j-th layer can be classified as the target signal s_i or not, where the value of c_{tn}^{j} is 1 or 0 respectively (when classified as s_i, the value of c_{tn}^{j} is 1, otherwise it is 0). At this point, we can classify different typical signals through different layers.

$$\mathbf{W}_j=\begin{bmatrix}\mathbf{w}_{MXN}(1)\\ \mathbf{w}_{MXN}(2)\\ \vdots\\ \mathbf{w}_{MXN}(T)\end{bmatrix} \tag{4}$$

$$\mathbf{C}_{TxN}^{j}=\text{Classifier}(\mathbf{W}_j)=\begin{bmatrix}\mathrm{c}_{11}^{j} & \mathrm{c}_{12}^{j} & \cdots & \mathrm{c}_{1N}^{j}\\ \mathrm{c}_{21}^{j} & \mathrm{c}_{22}^{j} & \cdots & \mathrm{c}_{2N}^{j}\\ \vdots & \vdots & \ddots & \vdots\\ \mathrm{c}_{T1}^{j} & \mathrm{c}_{T2}^{j} & \cdots & \mathrm{c}_{TN}^{j}\end{bmatrix} \tag{5}$$

C. Interlayer design

Another key to layer feature boosting is that the next layer will classify the residual signal that is retained from the previous layer.

From the perspective of the number of classified signals, since the target signal s_i is classified by the upper layer, s_i should be removed from the typical signal set in the following layer, and the number of typical signal sets in this layer is reduced compared to the upper layer. On the other hand, from the perspective of time series, according to the classification results of the upper level, the relevant sequences that have been classified as s_i can be truncated. The intercepted time series no longer contains data related to s_i, and it is consistent with the remaining signal types in the typical signal set. The relationship between the j-th layer and the $(j+1)$-th layer is shown in (6).

$$\mathbf{W}_j=\begin{bmatrix}\mathbf{w}_{M\mathrm{xN}}^{1}\\ \mathbf{w}_{M\mathrm{xN}}^{2}\\ \vdots\\ \mathbf{w}_{M\mathrm{xN}}^{T}\end{bmatrix}=\begin{bmatrix}\mathbf{A}_{M\mathrm{x}M}^{j}\cdot\mathbf{S}_{M\mathrm{xN}}+R(j+1)\\ \mathbf{A}_{M\mathrm{x}M}^{j}\cdot\mathbf{S}_{M\mathrm{xN}}+R(j+1)\\ \vdots\\ \mathbf{A}_{M\mathrm{x}M}^{j}\cdot\mathbf{S}_{M\mathrm{xN}}+R(j+1)\end{bmatrix}$$
$$\Big\downarrow \begin{array}{l}\text{After classifying a target signal } s_i\\ s_i \text{ occupies } a \text{ points in the time series}\end{array} \tag{6}$$
$$\mathbf{W}_{j+1}=\begin{bmatrix}\mathbf{w}_{(\mathrm{M-1})\mathrm{xN}}^{1}\\ \mathbf{w}_{(\mathrm{M-1})\mathrm{xN}}^{2}\\ \vdots\\ \mathbf{w}_{(\mathrm{M-1})\mathrm{xN}}^{T-a}\end{bmatrix}=\begin{bmatrix}\mathbf{A}_{(\mathrm{M-1})\mathrm{x(M-1)}}^{j+1}\cdot\mathbf{S}_{(\mathrm{M-1})\mathrm{xN}}+R(j+2)\\ \mathbf{A}_{(\mathrm{M-1})\mathrm{x(M-1)}}^{j+1}\cdot\mathbf{S}_{(\mathrm{M-1})\mathrm{xN}}+R(j+2)\\ \vdots\\ \mathbf{A}_{(\mathrm{M-1})\mathrm{x(M-1)}}^{j+1}\cdot\mathbf{S}_{(\mathrm{M-1})\mathrm{xN}}+R(j+2)\end{bmatrix}$$

From the above discussion, as the layer increases, the typical signal set and time series that enter each layer will gradually decrease. When reaching the later layers, the typical signal set will only contain the rare signal to be classified. Therefore, there will not be any sharp increase in the amount of computation caused by too many layers.

D. New features for anomaly detection in time series

In the establishment of the above model, this paper uses a typical data set $\mathbf{S}_{M\mathrm{xN}}(t)$. However, in actual pipelines, due to complexity factors of the environmental and hardware system, it is difficult to obtain consistent signals even if the same test piece is repeatedly tested. Therefore, it is inaccurate to directly use the typical data set to classify the target signal. Thus, it is more reliable to extract the features of typical signals and then use the meaning features to classify signals. In other words, $\mathbf{S}(t)$ in (1) will become:

$$\begin{aligned}\mathbf{S}&=[s_1\quad s_2\quad\cdots\quad s_{M-1}\quad s_M]^T\\ &\Big\downarrow\ \text{Extract Features}\\ \mathbf{F}&=\left[F_1\quad F_2\quad\cdots\quad F_{M-1}\quad F_M\right]^T\end{aligned} \tag{7}$$

where $\mathbf{F}$ represents the extracted feature matrix. F_i represents the feature vector extracted from the typical signal s_i. In the layer feature boosting framework, correct features selection at each level is important. The selected features of each layer need to identify the signals that match the selected features as much as possible. In addition, it is required to avoid missing data due to interfere with the next round of identification. At the same time, the features of each level are independent in which case there is no mutual interference of features between multiple layers that would result in uncertain classification.

Classifying defective signals from normal signals can be drawn as an anomaly detection problem. Time series anomaly detection is usually divided into two categories, namely point anomalies and anomaly series [23]. For these anomaly detections, a variety of time series features based on different dimensions are proposed. Statistical analysis treats time series as random variables, and uses statistics such as mean, variance, extreme value, quantile, slope and autocorrelation as the characteristics of time series. Another method is to use time series information in the temporal dimension as features, such as using a sliding window method to extract hour-level features or day-level features. However, statistical features that are based on global data statistics can obscure the impact of local outliers. While the temporal dimension feature takes into account local outliers, it cannot measure the impact of local changes on global variables. In addition, for temporal dimension features, the issue of selecting a time interval of a suitable length for subsequent feature establishment remains a challenge.

To solve the above problems, this paper also proposes a new structure feature that transforms the entire time series to two-dimensional polar coordinates. The length (i.e. magnitude) of the polar diameter direction measures the abnormal level of the point in the entire sequence (i.e., in a global sense), and the polar angle is used to indicate the abnormal level of the point in the local sequence (i.e., in a local sense) as depicted in Fig. 4.

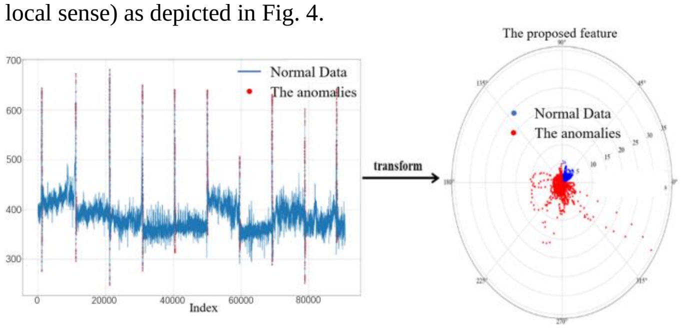

Fig.4 Example of the proposed feature in time series anomaly detection

For a long-term series, the normal value is usually stable within a normal range. Fig. 5 shows the normal range of a long-term time series. For a data point that lies outside the normal range, it can be considered that the cause of this data point has changed. For a data point that lies outside the normal range, it can be considered that the cause of this data point has changed.

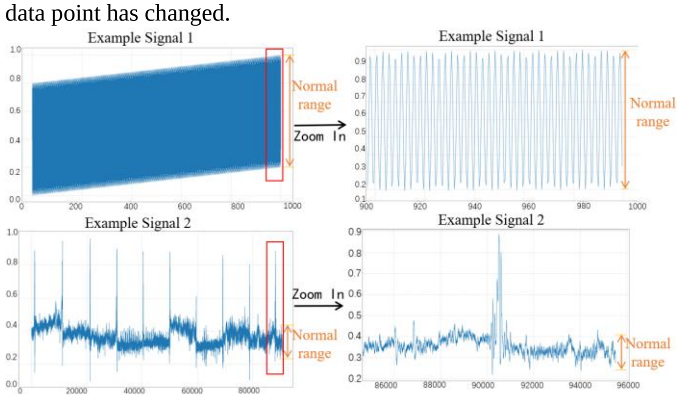

Fig.5 Normal range of some example signals

It can be considered that the cause of this data point has changed. In other words, the point may be an abnormal point. Therefore, the ratio of the amplitude of each point to the normal range of the sequence can be used to measure the degree of abnormality of a point. In addition, considering that the amplitude of anomalous points in certain sequences will have considerable leap of multiple times compared to the normal range of the sequence, the logarithm of their ratio is used to compress them so as to be displayed in the polar chart. Mathematically, features that measure the degree of global anomaly can be obtained as:

$$GF_{x_i} = 10 \cdot \log_{10}\left(\frac{Amp_{x_i}}{AMP_{nr}}\right) \tag{8}$$

In (8), GF is the abbreviation of global feature, the subscript x_i represents the *i-th* point on the time series. Amp_{x_i} represents the amplitude of x_i, and AMP_{nr} represents the normal range amplitude of the entire time series. With this global feature, the normal points will concentrate in a circle with a small radius after polar coordinate mapping, while abnormal points disperse on a circle with larger radius.

This paper adopts the use of polar angle in the polar coordinate system to reflect the local change rate of the time series. Given a time series $x_i (i = 1, 2, \cdots, n)$, a sliding window is used to extract its local feature sequence $LF_i (i = 1, 2, \cdots, n)$, as shown in Fig.6. The window length is specified as l where l points in the time series are sent to the feature extraction function $g(z)$ to obtain the feature value corresponding to the l-*th* point. Each time the window slides one point until the feature of the last point of the time series is obtained. Since it is necessary to ensure that the length of the feature sequence and the time sequence are equal, padding data with a length of $l-1$ is added to the head of the original time series. This is to ensure that it will not affect the future trend of the time series. The value is the first value of the time series to avoid the disturbance to the data caused by the additional value.

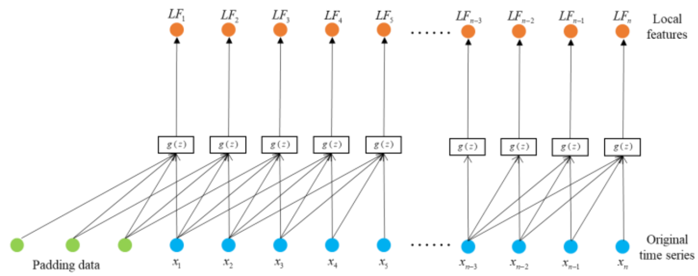

Fig.6 Schematic diagram of local feature extraction

In order to measure the local change rate of the time series, the feature extraction function $g(z)$ in each window computes the variance (given in (9)), normalize the value and convert it to radians according to (10) to obtain the polar angle. Using (10), the point with a small local rate of change can be mapped to the polar coordinate graph $[0, \pi/2]$, the point with a moderate rate of change is mapped to $[\pi/2, 3\pi/4]$, the points with a large rate of change are mapped to $[3\pi/4, 2\pi]$ part. If the standardized variance sequence is directly mapped, the points with small local rate of change will only occupy a very small part of the polar angle. This poses an issue where these variance features cannot be clearly detected on the feature map.

$$S^2 = \frac{\sum_{i=1}^{l}(x_i - \bar{x})^2}{l} \tag{9}$$

$$LF = \begin{cases} 4\pi \cdot Norm(S^2) & Norm(S^2) \le \frac{1}{8} \\ 2\pi \cdot Norm(S^2) + \frac{\pi}{4} & \frac{1}{8} \le Norm(S^2) \le \frac{1}{4} \\ \frac{1}{3}[5\pi \cdot Norm(S^2) + \pi] & Norm(S^2) \ge \frac{1}{4} \end{cases} \tag{10}$$

E. Loss function

For the data points detected by the eddy current sensor, each data point might belong to any of the multiple classification categories. Taking the signal in Fig. 3 as an example, there are five common categories that need to be identified in the pipeline, including normal, static, weld, bend, and defect. The loss function of each point can be defined as:

$$L_i = -\sum_{c=1}^{M} p_{ic} \log(p_{ic}) \tag{11}$$

where L_i represents the loss function of each point, M represents the types that may appear, and p_{ic} is the predicted probability of point i belonging to category c. The loss function of the entire time series can be defined as:

$$\begin{aligned} L &= L_{\text{Unclassified}} + L_{\text{Classified}} \\ &= \frac{1}{N}\left(\sum_i L_i + \sum_j L_j\right) \\ &= \frac{1}{N}\left(-\sum_i \sum_{c=1}^{M} P_{ic}\log(p_{ic}) + \sum_j P_{jc}\log(1)\right) \\ &= -\frac{1}{N}\sum_i \sum_{c=1}^{M} P_{ic}\log(p_{ic}) \end{aligned} \tag{12}$$

In (12), N is the length of the entire time series, and L represents the loss function of the entire time series, which is the sum of the classified time series loss function and the unclassified time series loss function. The number of points in the classified time series is j. Since it has been classified, the probability $p=1$, then $\log(p)$ is 0, while the classified loss function is 0. The number of points in the unclassified time series is i, and the loss function of the unclassified time series is obtained by adding the loss functions of i unclassified points. It should be noted that the classification results of the previous layer in the framework will cause the p_{ic} of the next layer to change, and each layer needs to be recalculated.

F. Quantitative Detectability Assessment

Since pipeline detection is a commercial service, the use of data is confidential and so far, there is no public dataset available. Therefore, this paper first builds a dataset. The constructed dataset contains not only the time series of various sensors collected by the inner detector, but also the label values for the defect signals and target signals.

If the label of a specific signal corresponds to the result and appears in the same position, it is considered that the signal corresponding to the position is classified correctly. In this paper, we use the F-score to estimate the detection capability of the algorithm. F-score can be expressed as:

$$F\text{-score} = (1+\beta^2)\cdot\frac{R\cdot P}{\beta^2\cdot P + R} \tag{14}$$

where P is precision and R is recall given by:

$$P = \frac{TP}{TP+FP} \tag{15}$$

$$R = \frac{TP}{TP+FN} \tag{16}$$

where TP is true positive, FP is false positive, FN is false negative, and TN is true negative. The value of β in the F-score will have an impact on accuracy and recall. For the pipeline inspection in this paper, we need to detect defects as much as possible to avoid potential safety hazards caused by missed inspections. Therefore, the recall is more important, so the value of β is adjusted to 2.

IV. Experiment and Result Analysis

A. Experimental Setup and Samples Preparation

Experiments have been carried out using the internal pipe pig system as described in Section II. The overall experiment is divided into two parts, the laboratory environment and the real pipe detection. As shown in Fig. 7(a), the eddy current probe is loaded on the XYZ's workbench and performs defect detection on the flat specimen. In Fig. 7(b), it illustrates the inner pipe pig system by machine pulling.

To verify the robustness of the proposed algorithm in the real environment, we have conducted experiments on oil pipelines in the real environment. As shown in Fig.7(c), the inner pipe pig is propelled by high pressure gas, and the running speed in the pipeline is around 0~10 m/s. The sampling frequency is 2344 Hz, and the minimum abnormal detection size can reach 4.27 mm.

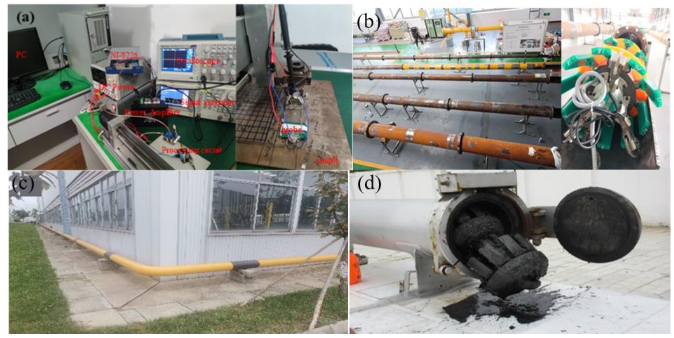

Fig.7 (a)Flat specimen detection. (b) Artificial pipe inspection. (c) Idle pipeline inspection. (d) Real pipe inspection.

Different specimens have been used in different environments and they are summarized in Table I. The first test data (shown in Table I specimen number 1) is collected from the laboratory environment. In the laboratory environment, a relatively ideal signal with less noise can be obtained. The tested samples are various flat test pieces or half-pipe test pieces engraved with artificial defects. The used sensor is only a single eddy current sensor. The purpose is to test the detection ability of the eddy current sensor for defects, and the ability of the algorithm to identify defects. During the test, we fix the eddy current sensor on the XYZ worktable to ensure that the probe sweeps across the surface of the specimen stably and uniformly under the premise of maintaining a fixed lift-off. After that, experiments are carried out in an artificial simulation environment as shown in Fig.7(b). In the artificial simulation environment, the inner detector is pulled by the motor, so that the inner detector moves at a constant speed of 0.5/m s in the pipeline. Many defects are engraved in the pipeline for the pulling experiment, and the specific location of the defects is known *a priori* for test validation. The welds exist between different pipe sections while the device used for signal acquisition is the internal detector as introduced in Section IV.

The second test data (shown in Table I specimen number 2,3) is collected from the artificial simulation experiment. Compared with the experiment in the laboratory environment, the signal has changed from single channel to multi-channel, and there exists more interference signals of the welding seam as well as different type of defects. At the same time, the movement speed of the inner detector is faster than that of the XYZ table. The difficulty of detection has increased.

Finally, the third test data (shown in Table I specimen number 4,5,6) is collected from the real environment. In the detection of the real environment, the inner detector is driven by high-pressure gas, and the speed cannot be controlled manually. Its running speed is 0~10/m s, and the speed change cannot be simulated in the first two environments. At the same time, compared with the artificial simulation environment, the real pipeline has new structures such as elbows, and the situation in the pipeline is more complex. There are potentially more dust and residual oil interference, which lead to large noise and therefore introduce huge challenges for accurate identification of defects. In particular, the exact location of the defects in the real pipeline is not known before detection, that is to say, it is not only required to successfully detect the defects, but it is also demanded to identify the accurate position of the defects, so as to facilitate the subsequent manual verification of the defect detection effect. The experiments in the real environment can be subdivided into two cases. In the first case, as shown in Fig.7 (c), the pipeline is an idle pipeline with a total length of around 200m and a total of 7 turns. Since the pipeline is idle, the inside of the pipeline is relatively clean and the signal quality is relatively low. In the second case, as shown in Fig.7(d), the oil and gas pipelines in actual use are detected. There are many impurities inside the pipelines, and the long-distance pipeline detection (up to 10km or more) causes high-pressure gas to push the inner detector. The forward momentum is insufficient, so the acquired signal is extremely noisy and jittery. In this paper, we will show the obtained results using verified data.

Table I Description of the experimental specimen

Parts	Specimen number	Pictures	Indication	Size	Defect information
Laboratory	1		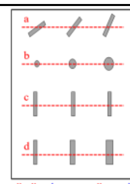	Unit: mm 250x250x10	a: Depth(mm):5 Angle(°):30/45/60 b: Depth(mm):4 Radius(mm):5/7/10 c: Depth(mm):4/6/8 d: Depth(mm):2 Width(mm):2/3/4
	2		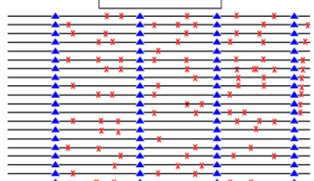	Radius: 35mm Length:367cm Thickness:7mm	See Appendix A for more details
	3	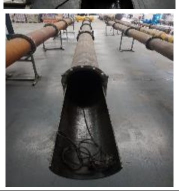	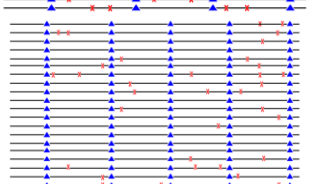	Radius: 43mm Length: 524cm Thickness:7mm	
Real Environment	4		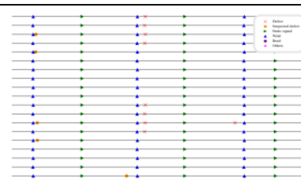	Radius: 35mm Length: 28.37m Thickness:7mm	/
	5		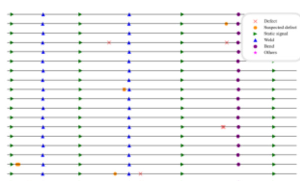	Radius: 35mm Length: 31.12m Thickness:7mm	
	6		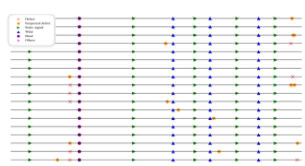	Radius: 35mm Length: 36.13m Thickness:7mm	

B. *Effects of the proposed feature*

Due to the complex environment in real pipelines, the quality of the signal acquired by the pig system is poor. In addition, it is difficult for the high-pressure gas to push the inner pig system stably and uniformly whereas the signal will appear irregular jitter. The above factors are unavoidable as they contribute interference to the detection of the defect signal. Traditional anomaly detection algorithms that use statistical features based on global data statistics will obscure the impact of local outliers. Since the temporal dimension feature takes into account local outliers, it cannot measure the impact of local changes on global variables. Additionally, for temporal dimension feature, the issue of selecting a time interval of a suitable length for subsequent feature establishment is a critical challenge.

The proposed feature map alleviates the above problems by determining a suitable tradeoff. In the first experiment, three anomaly detection algorithms i.e., iForest, OC-SVM, and Autoencoder, are selected. When the parameters of the same algorithm are controlled unchanged, the effect of recognition is shown in Fig. 8. Fig. 8 shows the prediction graphs of each classifier in two columns. The left column is the prediction result without adding the features proposed in this paper, and the right column is the prediction result after adding the feature. It is seen that the addition of features can not only detect abnormality normally, but also suppress the occurrence of false detection. Table II quantitatively analyzes the performance improvement of the three anomaly algorithms after adding the proposed feature. It can be seen from the table that for the three anomaly detection algorithms with completely different principles, the defect precision rate after adding the new feature has been improved, with a minimum improvement of 2.82 times and a maximum improvement of 13.33 times. The average increase is 4.97 times. According to the F-score, the three anomaly detection algorithms perform better.

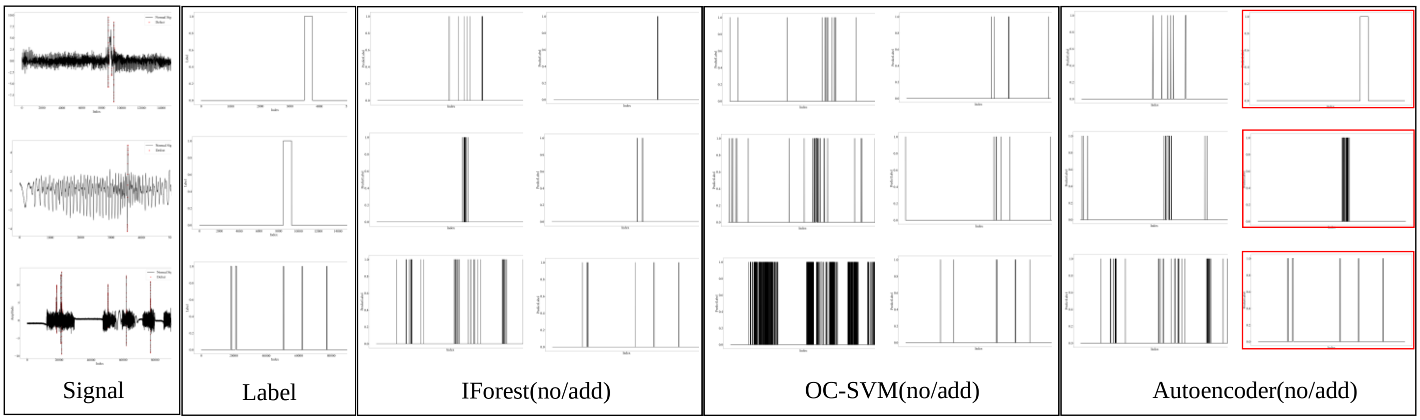

Fig.8 Schematic diagram of the influence of proposed features on anomaly detection algorithms

Table II The impact of proposed feature on anomaly detection algorithms

		iForest			OC-SVM			Autoencoder		
		Precision	recall	F-score	Precision	recall	F-score	Precision	recall	F-score
Signal 1	No feature	0.2	1	0.56	0.11	1	0.38	0.17	1	0.51
	Add feature	1	1	1	0.25	1	**0.625**	1	1	1
Signal 2	No feature	1	1	**1**	0.07	1	0.27	0.17	1	0.51
	Add feature	1	1	**1**	0.2	1	**0.56**	1	1	**1**
Signal 3	No feature	0.21	1	0.57	0.03	1	0.15	0.24	1	0.61
	Add feature	1	1	**1**	0.4	0.4	**0.4**	1	1	**1**

The data set in this paper is manually labeled, and the length of the label is affected by human factors. Different people have different criteria for determining the starting position of signals such as defects, welds, and elbows. Therefore, there might be differences between the prediction results of the model and the front as well as the rear positions of the corresponding labels.

If the evaluation is made in the way of point-to-point correspondence, there will be a large bias. Therefore, the undertaken experiment adopts the evaluation method of event-correspondence evaluation. If there are one or more predicted events within the range corresponding to the labeled event, it is considered that the labeled event has been successfully predicted. Otherwise, there is no such event, the interpretation is shown in Fig.9.

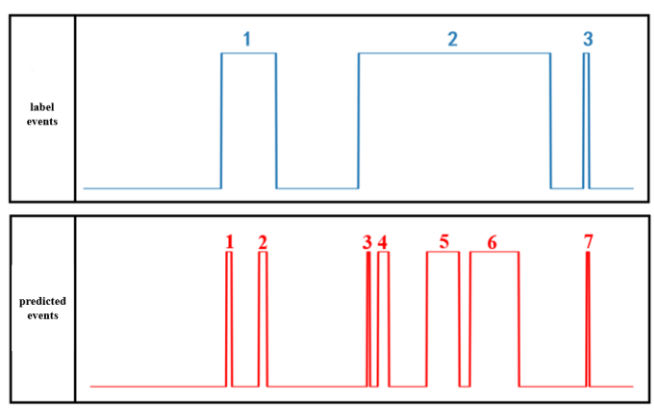

Fig.9 Relationship between labels and predicted events

In Fig.9, the blue line represents the tagging data that contains three tagging events. The red line represents the prediction result, and there are 7 corresponding prediction events in total. Since there are predicted events 1 and 2 at the corresponding positions of the marked event 1, the identification of the marked event 1 is successful detected.

Similarly, marked events 2 and 3 are identified successfully as well. In addition, the correctness of all indicators in this paper is based on the judgment of time.

C. Experiments Results and Discussion

The proposed training process is to construct a data set from all the detection data, and manually label it to obtain labeled data. Finally, K-fold cross-validation is used for training. Thus, a diverse range of different pipes as well as defects are covered in the training of model.

The proposed algorithm framework is to solve the abnormal identification of time series signals in pipeline non-destructive testing. Therefore, whether it is an oil pipeline or a natural gas pipeline, as long as the output detection signal is in the format of time series, the proposed framework can be readily used or adapted for such identification.

1) Real Pipe validation

The focus of laboratory experiments is to verify whether the algorithm can extract the required target signal according to the purpose in a relatively ideal environment. The experimental analysis in the laboratory environment can be viewed in Appendix B.

The experiments conducted in the laboratory serve to verify that our framework has a certain classification effect on complex pipeline signals. To further verify the robustness of the proposed framework, we will demonstrate the validity in detecting defects in oil pipelines in the real environment. Compared with the laboratory environment, the signals collected in the real pipe exhibit more complex behavior. There are environmental noise and mechanically-induced signals. There are also new structural parts such as bends. Therefore, the objective of the field experiment is to verify whether the proposed framework can achieve the ability of correctly classifying the target signal.

For real pipe signals, we have used the proposed three-layers feature boosting framework, and the detection result of specimen 4 in Table I is shown in Fig.10. The results of other specimens are shown in Appendix C. It is seen that the signal classified in the previous layer has been intercepted and will not be used as the input of the signal in the next layer. With the idea of multi-level classification, the target information in complex signals can be extracted step by step. The actual and predicted results for all specimens are shown in Appendix D, as a confusion matrix. It can be seen from the confusion matrix that for all types of anomalies (except for suspected defects), the recognition accuracy under the proposed framework is better.

The existing misidentification mainly occurs in the connection position of abnormal signal and normal signal whereas the proportion of misidentification is low. The category of suspected defects has a high misrecognition rate because there are few signals of this type in the model training. Although these are misidentified as defects, it is still acceptable within the industry standard since suspected defects are early signs of defects, and it is important to detect them early on.

When the defect detection is carried out directly without removing the weld signal, the signal amplitude of the weld is quite large compared to the defect other status signals. If the anomaly detection algorithms are directly applied, the weld will be falsely detected as a defect signal. At this time, defects and other status signals will be regarded as normal signals. As the contrast effect of (a) and (b) in Fig. 11, the red dots mark the detected abnormal signals.

Considering the case of after removing the weld signal, and the defect detection is carried out when the status signals are still present. Since the amplitude and waveform of the status signals are similar to the defect signal, the status signals will be mistakenly detected as a defect signal, resulting in the misidentification of defects, as shown in Fig 11 shown in (c) and (d).

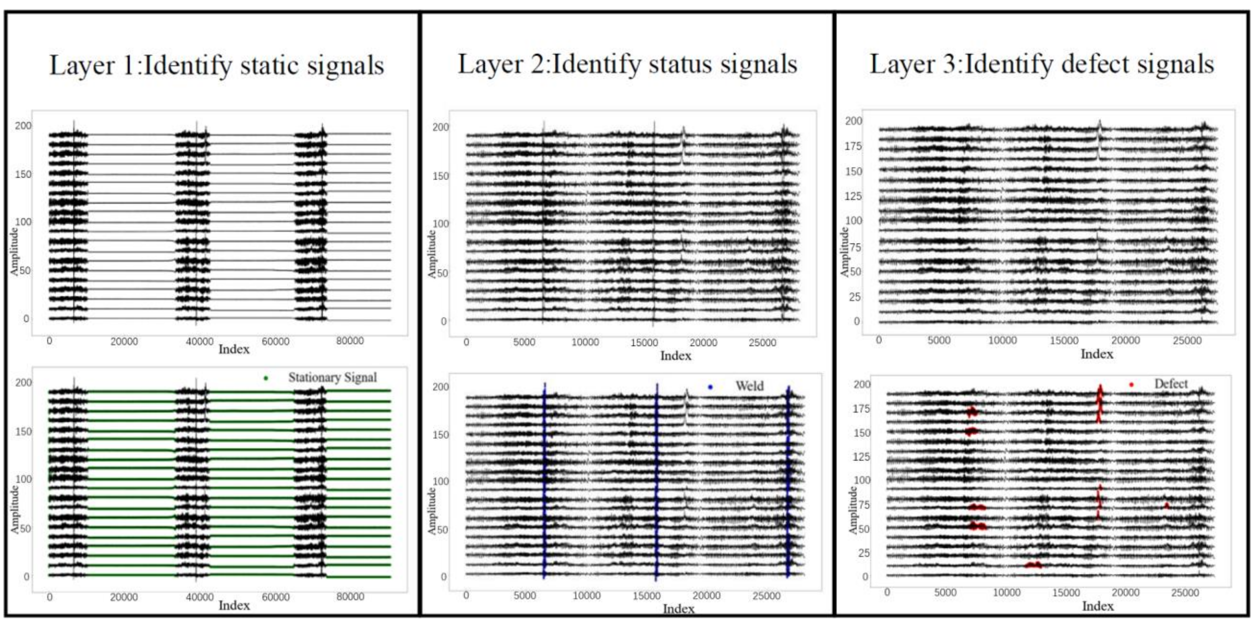

Fig.10 Schematic diagram of Feature Boosting applied to real pipeline detection

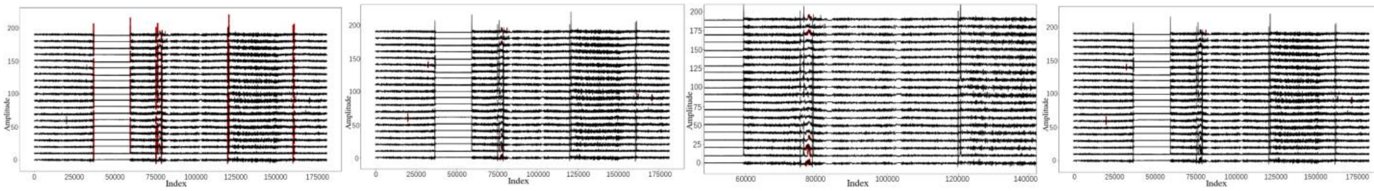

(a) (b) (c) (d)

Fig.11 (a) Defect detection without removing weld signal. (b) Defect detection under welding signal removal. (c) Defect detection without removing status signals. (d) Defect detection under the condition of removing status signals

2) *Comparison with other models*

According to several signals that often appear in the pipeline inspection, the multi-classified signals are determined as normal signals, static signals, weld signals, elbow signals, defect signals and suspected defect signals.

The multi-classification algorithms compared with our proposed framework include classical methods in machine learning (i.e., KNN, decision tree, Bayesian classifier, random forest), traditional neural networks in deep learning (i.e., MLP, LSTM), and Multi-Scale Convolutional Neural Networks (MSCNN) [24], which currently performs well in time series multi-classification. The selected comparison models in this paper range from the classical machine learning model to the state-of-the-art deep learning model which works well in multi-classification of the time series signal. These models are the optimal models obtained by training different types of signals through labeled data, and then compared with the proposed feature boosting model.

Using F-score with $\beta=2$ as the evaluation metric, the comparative effects of different multi-classification algorithms are shown in Table Ⅲ. It can be seen from Table Ⅲ that for the complex signals in the real pipeline, each classifier has a good recognition rate for signals with large amplitudes in the original time series such as static signals, weld signals, and bend signals. However, it is generally difficult to identify signals with small amplitudes in the original time series such as defect signals. Among them, Bayesian classifiers and LSTM-based multi-classification networks fail to identify the defect signals.

Our proposed method leverages the method of hierarchical classification of complex signals. Thus, it is shown to achieve better identification results for defect signals with small amplitudes. In addition, this structure also ensures that each layer is focused on detecting the target signal, which improves the precision rate and reduces the occurrence of missed detection events. Compared with KNN, which has the best effect in the multi-classification algorithms, our proposed framework not only guarantees the detection of static, weld, bend and other signals, but also the most relevant defect signals in practice with increased performance by more than 13%, and the detection of suspected defect signals increased by more than 41%.

Table Ⅲ F-values obtained from multi-classification algorithm processing field pipeline signals

	KNN	Decision Tree	Bayesian Classifier	Random Forest	MLP	LSTM	MSCNN	Ours
Normal signal	**1**	0.99	0.06	0.99	0.85	0.88	0.99	**1**
Defect signal	0.62	0.46	0	0.54	0.20	0	0.49	**0.70**
Suspected defect signal	0.27	0.17	0	0.24	0.11	0	0.29	**0.38**
Static signal	**1**	1	0.92	1	0.95	0.96	0.97	0.99
Weld signal	**1**	0.74	0.13	0.62	0.93	0.70	0.77	0.91
Bend signal	**1**	0.98	0.88	1	0.64	0.93	0.74	0.86

V. Conclusion

This paper has proposed a time-series anomaly detection framework based on feature boosting. The framework extracts the target signal layer by layer for the complex signals, and realizes the automatic detection of defects in the real pipeline signal. The multi-classification experiments of real signals show that the proposed framework has a positive effect on identifying various target signals in complex signals. In addition, the proposed new feature considers the global information as well as the local information of time series signals, which significantly improves the anomaly detection effect of time series.

V. ACKNOWLEDGEMENT

The work was supported by Deyuan and UESTC Joint Research Center, supported by the National Natural Science Foundation of China (No. 61971093 and No. 61527803), supported by the International Science and Technology Innovation Cooperation Project of Sichuan Province: 2021YFH0036, Science and Technology Department of Sichuan, China (Grant No.2018JY0655 and Grant No.2018GZ0047)

VI. References

[1]. Shumway R H, Stoffer D S, Stoffer D S. Time series analysis and its applications[M]. New York: Springer, 2000. P. 8.

[2]. Ester M, Kriegel H P, Sander J, et al. A density-based algorithm for discovering clusters in large spatial databases with noise[C]//kdd. 1996, 96(34): 226-231.

[3]. Breunig M M, Kriegel H P, Ng R T, et al. LOF: identifying density-based local outliers[C]//Proceedings of the 2000 ACM SIGMOD international conference on Management of data. 2000: 93-104.

[4]. Liao Y, Vemuri V R. Use of k-nearest neighbor classifier for intrusion detection[J]. Computers & security, 2002, 21(5): 439-448.

[5]. Tax D M J, Duin R P W. Support vector data description[J]. Machine learning, 2004, 54(1): 45-66.
[6]. Wang D, Yeung D S, Tsang E C C. Structured one-class classification[J]. IEEE Transactions on Systems, Man, and Cybernetics, Part B (Cybernetics), 2006, 36(6): 1283-1295.
[7]. Pang J, Pu X, Li C. A Hybrid Algorithm Incorporating Vector Quantization and One-Class Support Vector Machine for Industrial Anomaly Detection[J]. IEEE Transactions on Industrial Informatics, 2022.
[8]. Liu F T, Ting K M, Zhou Z H. Isolation-based anomaly detection[J]. ACM Transactions on Knowledge Discovery from Data (TKDD), 2012, 6(1): 1-39.
[9]. Guha S, Mishra N, Roy G, et al. Robust random cut forest based anomaly detection on streams[C]//International conference on machine learning. PMLR, 2016: 2712-2721.
[10]. Wu D, Jiang Z, Xie X, et al. LSTM learning with Bayesian and Gaussian processing for anomaly detection in industrial IoT[J]. IEEE Transactions on Industrial Informatics, 2019, 16(8): 5244-5253.
[11]. Jang K, Hong S, Kim M, et al. Adversarial Autoencoder Based Feature Learning for Fault Detection in Industrial Processes[J]. IEEE Transactions on Industrial Informatics, 2021, 18(2): 827-834.
[12]. Liu Y, Li Z, Zhou C, et al. Generative adversarial active learning for unsupervised outlier detection[J]. IEEE Transactions on Knowledge and Data Engineering, 2019, 32(8): 1517-1528.
[13]. Yu M, Sun S. Policy-based reinforcement learning for time series anomaly detection[J]. Engineering Applications of Artificial Intelligence, 2020, 95: 103919.
[14]. Zhao H, Wang Y, Duan J, et al. Multivariate time-series anomaly detection via graph attention network[C]//2020 IEEE International Conference on Data Mining (ICDM). IEEE, 2020: 841-850.
[15]. Xiao N H. New Technologies and Technical Standards for Modern Non-Destructive Testing Technology and Application[J]. Beijing Silver Sound Audiovisual Press: Beijing, China, 2004.
[16]. Piciarelli C, Avola D, Pannone D, et al. A vision-based system for internal pipeline inspection[J]. IEEE Transactions on Industrial Informatics, 2018, 15(6): 3289-3299.
[17]. Ma Q, Tian G, Zeng Y, et al. Pipeline In-Line Inspection Method, Instrumentation and Data Management[J]. Sensors, 2021, 21(11): 3862.
[18]. Sophian A, Tian G Y, Taylor D, et al. Electromagnetic and eddy current NDT: a review[J]. Insight, 2001, 43(5): 302-306.
[19]. Gupta K, Ghasr M T, Kharkovsky S, et al. Fusion of Microwave and Eddy Current Data for a Multi‐Modal Approach in Evaluating Corrosion Under Paint and in Lap Joints[C]//AIP Conference Proceedings. American Institute of Physics, 2007, 894(1): 611-618.
[20]. Sophian A, Tian G Y, Taylor D, et al. A feature extraction technique based on principal component analysis for pulsed Eddy current NDT[J]. NDT & e International, 2003, 36(1): 37-41.
[21]. Earnest J W. An Algorithm for Automated Feature Detection of Eddy Current Defects Using Sum of Gaussian Method[J]. IEEE Transactions on Instrumentation and Measurement, 2021, 70: 1-8.
[22]. D'Angelo G, Laracca M, Rampone S. Automated Eddy Current non-destructive testing through low definition lissajous figures[J]. 2016 IEEE Metrology for Aerospace (MetroAeroSpace), 2016: 280-285.
[23]. Blázquez-García A, Conde A, Mori U, et al. A review on outlier/anomaly detection in time series data[J]. arXiv preprint arXiv:2002.04236, 2020.
[24]. Cui Z, Chen W, Chen Y. Multi-scale convolutional neural networks for time series classification[J]. arXiv preprint arXiv:1603.06995, 2016.

Hewu Xu received the B.Sc. degree from the University of Electronic Science and Technology of China (UESTC) in 2019 and the M.Sc. degree from UESTC in 2021. His research interests include time series anomaly detection and machine learning.

Yupei Yang received the B.Sc. degree from the University of Electronic Science and Technology of China (UESTC), Chengdu, China, in 2019. He is currently pursuing the M.Sc. degree in nondestructive testing using eddy current technique with the University of Electronic Science and Technology of China, Chengdu. His research interests include eddy current testing and wireless energy transfer.

Bin Gao (M' 12-SM' 14) received his B.Sc. degree in communications and signal processing from Southwest Jiao Tong University (2001-2005), China, MSc degree in communications and signal processing with Distinction and PhD degree from Newcastle University, UK (2006-2011). He worked as a Research Associate (2011-2013) with the same university on wearable acoustic sensor technology. Currently, he is a Professor with the School of Automation Engineering, University of Electronic Science and Technology of China (UESTC), Chengdu, China. His research interests include electromagnetic and thermography sensing, machine learning, nondestructive testing and evaluation where he actively publishes in these areas. He is also a very active reviewer for many international journals and long standing conferences. He has coordinated several research projects from National Natural Science Foundation of China. Personal web: http://faculty.uestc.edu.cn/gaobin/zh_CN/lwcg/153392/list/index.htm

Xiangyu Zhao received the B.Sc. degree from the Southwest Minzu University, Chengdu, China, in 2020. She is currently pursuing the M.Sc. degree in nondestructive testing using eddy current technique with the University of Electronic Science and Technology of China, Chengdu. Her research interests include machine learning and anomaly detection..

Wai Lok Woo (M'11–SM'12) received the B.Eng. degree in electrical and electronics engineering, and the M.Sc. and Ph.D. degrees in statistical machine learning from Newcastle University, U.K., in 1993, 1995, and 1998, respectively. He was the Director of research for the Newcastle Research and Innovation Institute, and the Director of operations for Newcastle University. He is currently a Professor of Machine Learning with Northumbria University, U.K. He has published more than 400 papers on these topics on various journals and international conference proceedings. His research interests include the mathematical theory and algorithms for data science and analytics, artificial intelligence, machine learning, data mining, latent component analysis, multidimensional signal, and image processing. He is a Member of the Institution Engineering Technology. He was a recipient of the IEE Prize and the British Commonwealth Scholarship. He serves as an Associate Editor to

several international signal processing journals, including IET Signal Processing, the Journal of Computers, and the Journal of Electrical and Computer Engineering